



OPEN

Bi-HPDO3A as a novel contrast agent for X-ray computed tomography

Rebecca Rizzo¹, Martina Capozza¹, Carla Carrera² & Enzo Terreno¹✉

A new bismuth-based CT agent was synthesized through a facile synthesis strategy. The in vitro stability, toxicity and CT performance were evaluated. The in vivo imaging performance was investigated using three different doses (0.5, 1.2 and 5 mmol/kg) and the result obtained at 1.2 mmol/kg was compared with the clinically approved CT agent iopamidol at the same dosage.

Bismuth is a naturally monoisotopic (²⁰⁹Bi) element that is commonly considered the heaviest stable element of the Periodic Table due to the extremely long theoretical half-life of 1.9×10^9 years¹. Over the years, bismuth have found many applications in different fields starting from the preparation of non-toxic pigments and catalysts, the synthesis of biocompatible additives in dental materials², and the development of therapeutics against *H. pylori* infections or in the treatments of ulcera gastritis and dyspepsia³. More recently, bismuth compounds have also been demonstrated active against coronavirus including both SARSCoV-1 and SARS-CoV-2, through the inhibition of a zinc enzyme helicase⁴. The biomedical applications of Bi were further implemented in the fields of imaging, cancer treatment, drug delivery and biosensing⁵. Beside the natural isotope ²⁰⁹Bi, the artificial ²¹²Bi and ²¹³Bi radioisotopes have been recently attracting interest as potential therapeutic radionuclides in targeted alpha therapy⁶. Especially, the nuclear properties of ²¹³Bi are very suited for dosimetry studies and/or to monitor the biodistribution of the nuclide using single photon emission computed tomography (SPECT)⁷. However, Bi shows the highest X-ray absorption among the heavy metals at any energy of incident X-ray photons, thus making it a perfect candidate for designing X-ray Contrast Agents (XCAs)⁸. Moreover, Bi-compounds exhibit relatively low toxicity, when compared to other heavy metals⁵. Computed tomography (CT) has been widely employed in both medical and non-medical applications since the discovery of X-rays in 1895⁹. The technique relied on X-rays absorption by matter and the X-ray attenuation depends on tissues composition, in particular density and atomic number of the tissue components¹⁰. Whereas CT imaging of hard tissues such as bones and cartilages are very sensitives to X-rays, imaging of soft structures (fatty tissues or neoplastic formations) required contrast agents to improve the image performance¹¹. Currently, the use of a CT agent requires the administration of the probe in the molar range, which represents one of the major downsides of this diagnostic tool compared to other imaging techniques such as MRI (sub-molar conc. range), nuclear and optical imaging (μmolar conc. range)¹⁰, especially in the field of molecular imaging. CT contrast agents are based on high-Z elements and may be classified in two major categories: small molecular agents (typically based on iodine or lanthanides) and nanoparticulate agents. Although iodine (Z = 53) has historically been the atom of choice for CT imaging applications, clinically employed iodinated contrast agents (e.g., iohexol, ioversol, and iopamidol) suffer from low sensitivity, poor spectral CT, potential allergy, and renal toxicity^{12–14}. Hence, the development of improved CT contrast agents is still subject matter of interest. To date, the development of Bi-based CT agents is mostly focused on the design of nanoparticle systems because of their greater contrast density, longer circulation times and versatility for targeting purposes¹¹. Representative examples are the Bi₂S₃ nanoparticles labelled with the cyclic nine amino acids peptide LyP-1 for targeting breast cancer¹³ and the MUC-16 aptamer targeted Bi-DOTA-PEG nanoparticles for imaging cervical cancer¹⁴. However, despite the promising preclinical results, no clinical translation has been reported so far for nanoparticulate agents, unlike small metal chelate-based contrast agents. On the other side, Bi-based small molecules have not been still sufficiently emphasized, with just a few examples reported, such as Bi-DPTA¹⁵ and Bi-DOTA¹⁶. On these premises, the aim of this study is to develop a new potential Bi-based small complex using the ligand HPDO3A (Fig. 1). HPDO3A is successfully used in MRI clinical exams since 2003, when its Gd(III) complex (Gadoteridol, marketed as ProHance[®]) received the approval for clinical use. A very important advantage of Bi-HPDO3A over the previously reported Bi-DOTA and Bi-DTPA complexes, is represented by its electroneutrality that may allow the administration of a higher dosage without affecting the

¹Department of Molecular Biotechnology and Health Sciences, Molecular Imaging Centre, University of Torino, Via Nizza 52, 10126 Turin, Italy. ²Institute of Biostructures and Bioimaging, National Research Council, Via Nizza 52, 10126 Turin, Italy. ✉email: enzo.terreno@unito.it

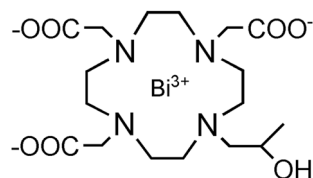


Figure 1. Bi-HPDO3A chemical structure.

osmolarity of the injected solution, and, as it has been clearly demonstrated for the complexation of lanthanide ions, without reducing the thermodynamic and kinetic stabilities of the metal complex¹⁷. The synthesis of Bi-HPDO3A is simple and cost-effective, and the ligand can be easily modified to allow the conjugation of the complex to targeting vectors¹⁸. In this work, the newly proposed agent has been characterized both *in vitro* and *in vivo* in terms of biocompatibility and CT imaging performance, using iopamidol as reference.

Experimental section

Chemicals

All chemicals were purchased from Sigma-Aldrich, all the solvents from VWR, HPDO3A and Iopamidol (Isovue 370) were kindly provided by Bracco Imaging S.p.A.

Electrospray ionization (ESI)-mass spectrometer (ESI-MS) of Bi-HPDO3A was obtained on Waters system (3100 Mass Detector, 2525 quaternary pump, 2767 sample manager, 2996 PDA detector). ¹H-NMR spectra and ¹³C-NMR spectra were measured on a Bruker Avance spectrometer (600 MHz) instrument. Chemical shifts are reported in parts per million (ppm) and are referenced to tetramethylsilane.

UV/Vis spectrophotometric measures were performed on a UV/Vis spectrophotometer (6715, Jenway).

Cell cultures and animals

Monocyte-macrophages (J774 cells) were purchased from ATCC. Cells were cultured until confluence using DMEM (Euroclone) medium supplemented with glutamine (2 mM), 10% fetal bovine serum (FBS, Sigma-Aldrich, St. Louis, MO, USA) and penicillin/streptomycin antibiotics (10,000 IU/mL penicillin, 10,000 IU/mL streptomycin, Corning Cellgro, Manassas, VA). MTT Cell Proliferation Kit was purchased from OZ Bioscience.

5-weeks-old BALB/C male mice were obtained from the animal facility of the Department of Molecular Biotechnology and Health Sciences (University of Turin, Italy). Animal manipulation and experimental procedures were carried out in accordance with the European Community guidelines (directive 2010/63) and under the approval of the Italian Ministry of Health (authorization #229/2016).

Synthesis and characterization of Bi-HPDO3A

Bi-HPDO3A complex was synthesized starting from HPDO3A ligand and bismuth(III) carbonate in a 2:1 molar ratio, respectively (Fig. 2). 1 g (2.36 mmol) of ligand was solubilized in 15 mL of deionized water prior to bismuth carbonate addition (0.75 g, 1.18 mmol) and the mixture was heated at 95 °C for 3 weeks. The xylenol orange test was performed to monitor the reaction progress and a small amount of ligand was added to have a free metal quantity not exceeding 0.1%. The reaction suspension was filtered (0.45 μm pore size) and the filtrate was lyophilized to obtain a white solid. The compound was then used without further purification.

The metal chelate was characterized by ¹H-NMR, UV-Vis spectrophotometry, and ultra-performance liquid chromatography-mass spectrometry (UPLC-MS). The new bismuth agent was dissolved in deionized water and diluted to the concentration of 0.4 mM for UV/Vis measurements (200–500 nm range). For NMR characterization, the complex was dissolved in D₂O to a final concentration of 3 mg/mL and, the ¹H- and ¹³C-NMR spectra were acquired at room temperature. The complex was also characterized by ESI-MS, and UPLC-UV/Vis spectra were recorded to assess the purity.

Stability measurements over time and transmetallation with Zn(II)

Physical stability of an aqueous solution of the complex was checked within 14 days to assess colloids formation. Stability in PBS and human serum at 37 °C was monitored within 24 h by measuring the absorbance of the Bi-complex (0.123 M) at 305 nm at 3 different times (3, 6 and 24 h). Transmetallation of Bi-HPDO3A towards

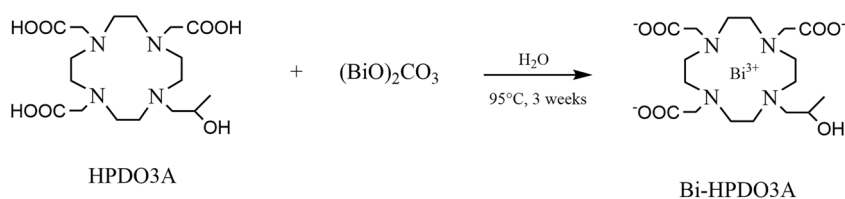


Figure 2. Bi-HPDO3A synthetic procedure.

Zn(II) ions was investigated by measuring the absorbance of the Bi-complex at 305 nm at 3 different times (3, 6 and 24 h) after mixing equimolar amount (20 mM) of Bi-HPDO3A and Zn(II) at 37 °C and pH 7.4.

In vitro cytotoxicity

Cellular methyl thiazolyl tetrazolium (MTT) assay was carried out to evaluate the cytotoxicity of Bi-HPDO3A in vitro. J774 cells (50 k cells/well) were incubated in a 96-wells plate for 24 h. The medium was then replaced by fresh one containing different concentrations of Bi-HPDO3A (3, 6, 12.5, 25, 50, 125, 250, and 500 μM). After the incubation, cells were incubated with MTT reagent for 3 h. Then, the solubilization solution was added to dissolve the purple formazan crystals. After 30-min of mild shaking, the absorbance value at 600 nm of each well was recorded through a microplate reader. The experiment was conducted in triplicate in 3 different experimental sessions.

CT imaging

Aqueous solutions at different Bi-HPDO3A concentrations (3–400 mM range) were prepared, and in vitro CT imaging was performed (MiLabs VECTOr⁶, 65 kV, 0.25 mA, 45 ms). A commercially available solution of iopamidol (Isovue-370[®] Bracco Imaging), properly diluted, was used as reference.

For in vivo CT imaging experiments, mice were anaesthetized with isoflurane (1.5–2.5%, 1 mL/min oxygen flow rate) and then scanned before and after the injection via the tail vein of 100 μL of Bi-HPDO3A or iopamidol solutions to reach a dose of 0.5, 1.2 and 5 mmol Bi/kg bw or 1.2 mmol I/kg bw, respectively. CT scans were acquired at different time points (0, 1 min, 5 min, 20 min, 40 min, 1 h). The parameters were set as follows: field of view 54 × 140 mm, tube current 0.25 mA, tube voltage 65 kV, exposure time 45 ms. VOIs analysis for kidneys and bladder were performed to semi-quantify the complex distribution in these main involved organs.

Histology

To verify possible acute toxicity effects of Bi-HPDO3A on kidneys, hematoxylin–eosin (HE) staining was carried out on mice kidneys explanted 7 days and 14 days after the administration of the agent (5 mmol Bi/kg bw).

Ethical approval

The study is reported in accordance with ARRIVE guidelines.

Results and discussion

Synthesis and characterization of Bi-HPDO3A

The Bi-HPDO3A complex was characterized by multiple analytical methods. The ¹H-NMR spectra (600 MHz, D₂O, pH 6.5, 298 K) of Bi-HPDO3A was characterized by the following signals (TMS as reference): 1.19 ppm (d, 3H, methyl group), 3.10–3.67 ppm (m, 19H, ethyl groups), 3.81 ppm (m, 3H, ethyl group), 4.05 ppm (d, 1H, hydroxyl), 4.36–4.49 ppm (m, 3H, ethyl group) (See Supplementary Information Fig. S3).

The ESI-MS spectrum of Bi-HPDO3A was characterized by m/z peaks found at 306.02, 611.16 and 1221.44, which correspond to [M+2H]²⁺, [M+H]⁺ and [2M+H]⁺, respectively. Furthermore, as calculated from the UPLC-UV/Vis spectrum, the metal complex was obtained with a purity > 99%. See Supplementary Information (Figs. S1, S2).

In vitro stability

Colloidal stability of a solution of Bi-HPDO3A 0.123 M (1.2 mmol/kg) was checked within 14 days after storage at room temperature. The solution remained clear without any precipitation event after centrifugation at 4000 rpm for 10 min. Structural stability of the bismuth complex was investigated by means of UV-Vis measurements. The complex proved to remain intact both in PBS and HS for 24 h at 37 °C (Fig. S11). Crucial aspect to be considered for the potential clinical translation of a metal complex is to check the stability towards transmetallation. Due to the relatively high blood concentration (55–125 μM) and the high affinity to polyamino-polycarboxylic ligands, Zn(II) is typically used as competitor endogenous metal ion to predict the in vivo stability of metal complexes¹⁹.

A calibration curve was preliminary assessed for Bi-HPDO3A (Fig. S4) and the whole UV-Vis spectrum was recorded to establish the maximum absorption wavelength (λ_{max} , 305 nm) of the complex. Figure 3 indicates that the absorbance of Bi-HPDO3A at 305 nm in presence of an equimolar amount of Zn(II) ions was not affected after one day of incubation at 37 °C and pH 7.4. This result fully agrees with the high thermodynamic and kinetic stability expected for Bi-HPDO3A complex. In fact, it has been reported that Bi(III) forms octacoordinated highly stable complexes and log K_{ML} values of 30.3 and 26.8 have been reported for DOTA and an HPDO3A-like ligand, respectively²⁰.

Cytotoxicity

The cytotoxicity of Bi-HPDO3A was assessed by the standard MTT test on a murine cell line of macrophages (J774). Cells were incubated for 24 h with different concentrations of the Bi-complex (0–500 μM range).

The result of the MTT test (Fig. 4) revealed an excellent biocompatibility with cell viability values attesting from 90 to 100% with no statistically significant differences (statistical analyses were conducted using the one-way ANOVA method and statistical significance was defined at P values less than 0.05) in the examined concentration range except for the concentration of 500 μM.

In vitro CT imaging performances

The in vitro CT performance of Bi-HPDO3A was evaluated by measuring the X-ray attenuation as a function of the probe concentration in the 0–400 mM range (Fig. 5). Data were compared with solutions of iopamidol

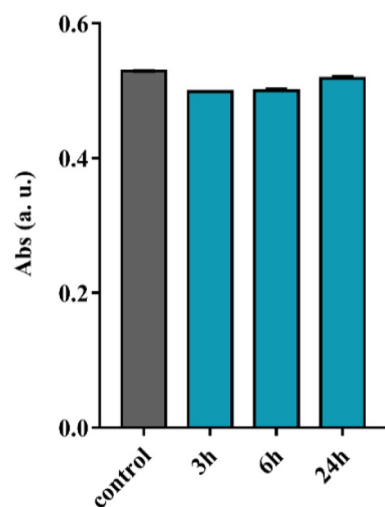


Figure 3. UV measurements at $\lambda = 305$ nm for transmetalation study of Bi-HPDO3A (20 mM) with Zn^{2+} (20 mM).

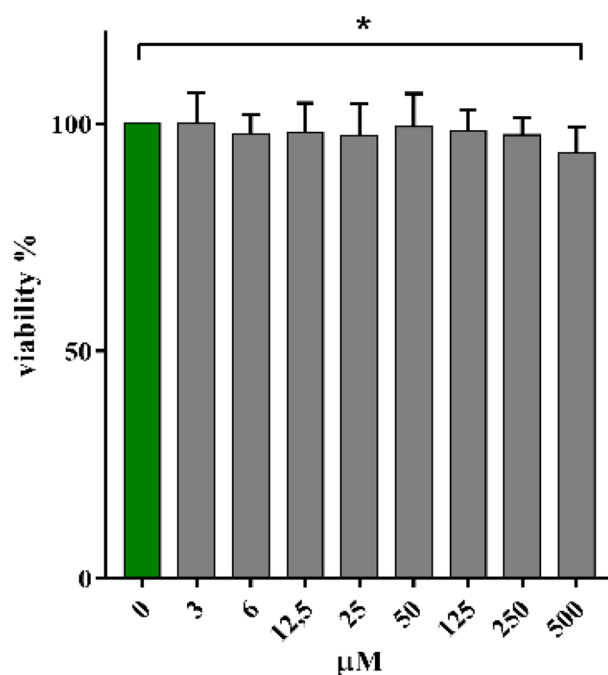


Figure 4. Viability % on J774 cells treated with Bi-HPDO3A (24 h, 0–500 μM). $P^* = 0.044$.

containing iodine concentrations in the same interval. The expected linear correlation between HU units and atom concentration was found for both agents. Unfortunately, the voltage limitations imposed by the available scanner (65 kV) prevented to exploit the larger X-ray attenuation coefficient of Bi at higher voltage, and in this acquisition setting, the two agents performed very similarly.

In vivo CT imaging experiments and toxicity assessment

The promising properties observed in vitro for Bi-HPDO3A prompted us to preliminarily test the in vivo performance of the agent on healthy mice.

The first dosage of 5 mmol/kg of Bi-HPDO3A were intravenously injected into BALB/C mice to assess biodistribution and in vivo X-ray attenuation capability of the agent. A high CT contrast was observed both in kidneys and bladder (Fig. 6A,B). Kidneys were already lighted up 1-min post injection, and within 60 min the bladder CT contrast signal increased linearly. Interestingly, after a rapid increase, the enhancement of the renal signal remained largely unchanged after 20 min post injection. Encouraged from this positive result, a lower

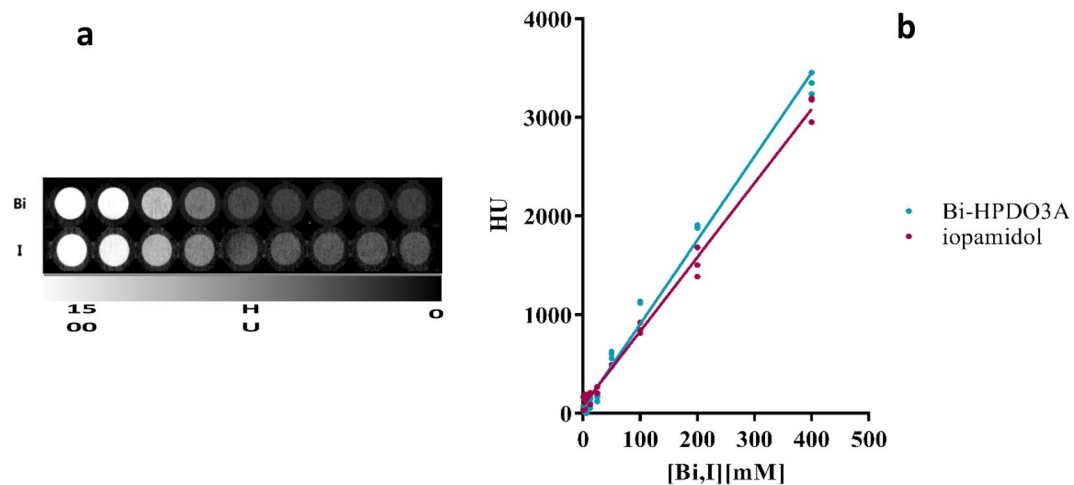


Figure 5. (a) Phantom CT imaging. (b) Comparison between Bi-HPDO3A and iopamidol in vitro CT attenuation capabilities.

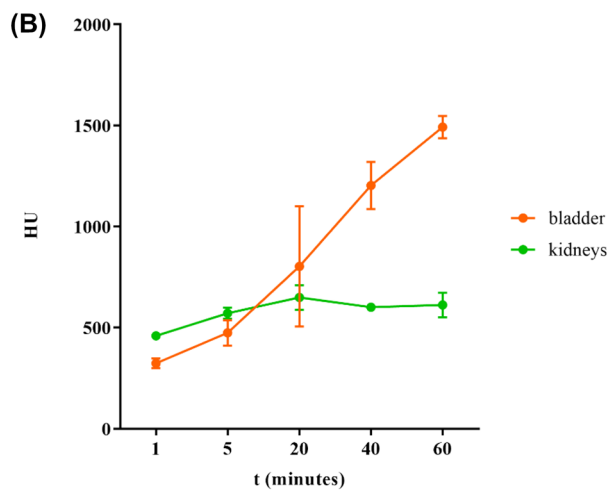
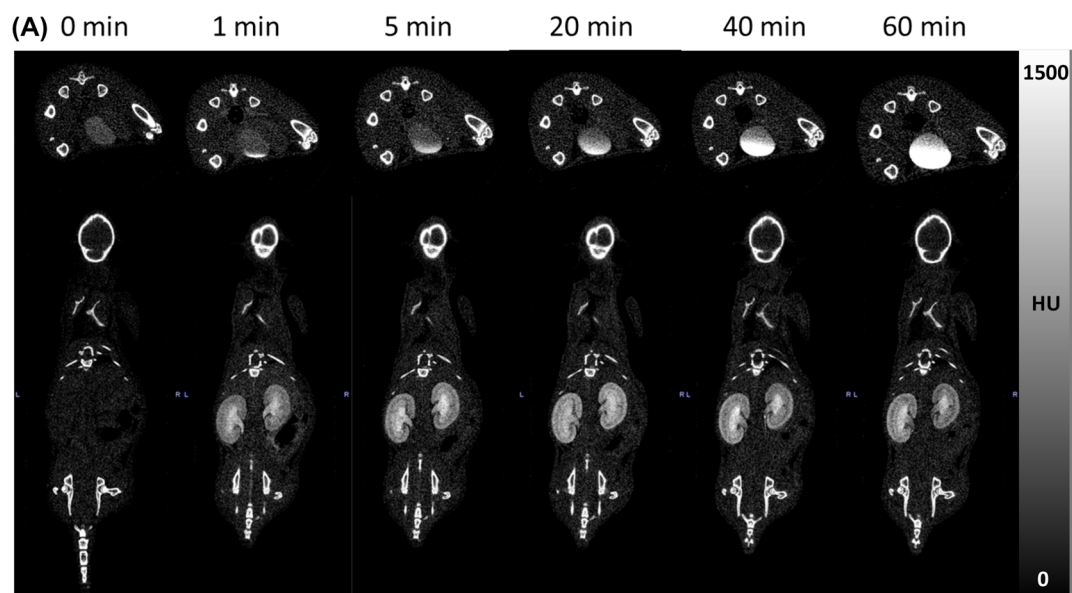


Figure 6. (A) In vivo CT imaging after *i.v.* administration of 5 mmol/kg of Bi-HPDO3A. Bladder and kidneys CT contrast are displayed. (B) VOI analysis on bladder and kidneys for a dose of 5 mmol/kg of Bi-HPDO3A.

injected dose (1.2 mmol/kg) was tested. This value was calculated starting from the clinical injected dose of the MRI agent Gadoteridol, scaled down to mice, taking into account the difference in body surface area between the two organisms²¹. Despite the expected lower CT contrast, a clear signal was detected in the renal collecting system (calyx and ureter, Fig. 7A,B, Fig. S4). To further challenge the attenuation capability of the Bi-HPDO3A complex, a further dose reduction (down to 0.5 mmol/kg) was attempted (Fig. S6). Expectedly, the CT contrast was the lowest among the three conditions explored, and the signal decreased according to the dose (Fig. 8). The signal was only detected on the calyx portion of the collecting system with a maximum peak 5-min post injection to finally disappeared 40-min post injection.

For comparative purposes, the imaging performance of Bi-HPDO3A was challenged with the clinically approved iodine-based iopamidol, using the injected dose of 1.2 mmol/kg. Iopamidol allowed for the visualization of the whole renal region (Fig. S8a) and, when compared to Bi-HPDO3A, displayed a slower renal clearance (Fig. S8b) with the kidney contrast that progressively increased in the first hour post-injection, in agreement with literature data²².

The different contrast dynamics displayed by the two probes in the kidneys is reported in Fig. 8.

Considering that the amount of the injected probes was equal, the higher contrast detected for iopamidol is primarily due to the higher molar concentration of attenuating atoms (3 iodine atoms/molecule vs 1 Bi atom/molecule), whereas the different dynamics can be explained in terms of the different hydrophilicity of the two

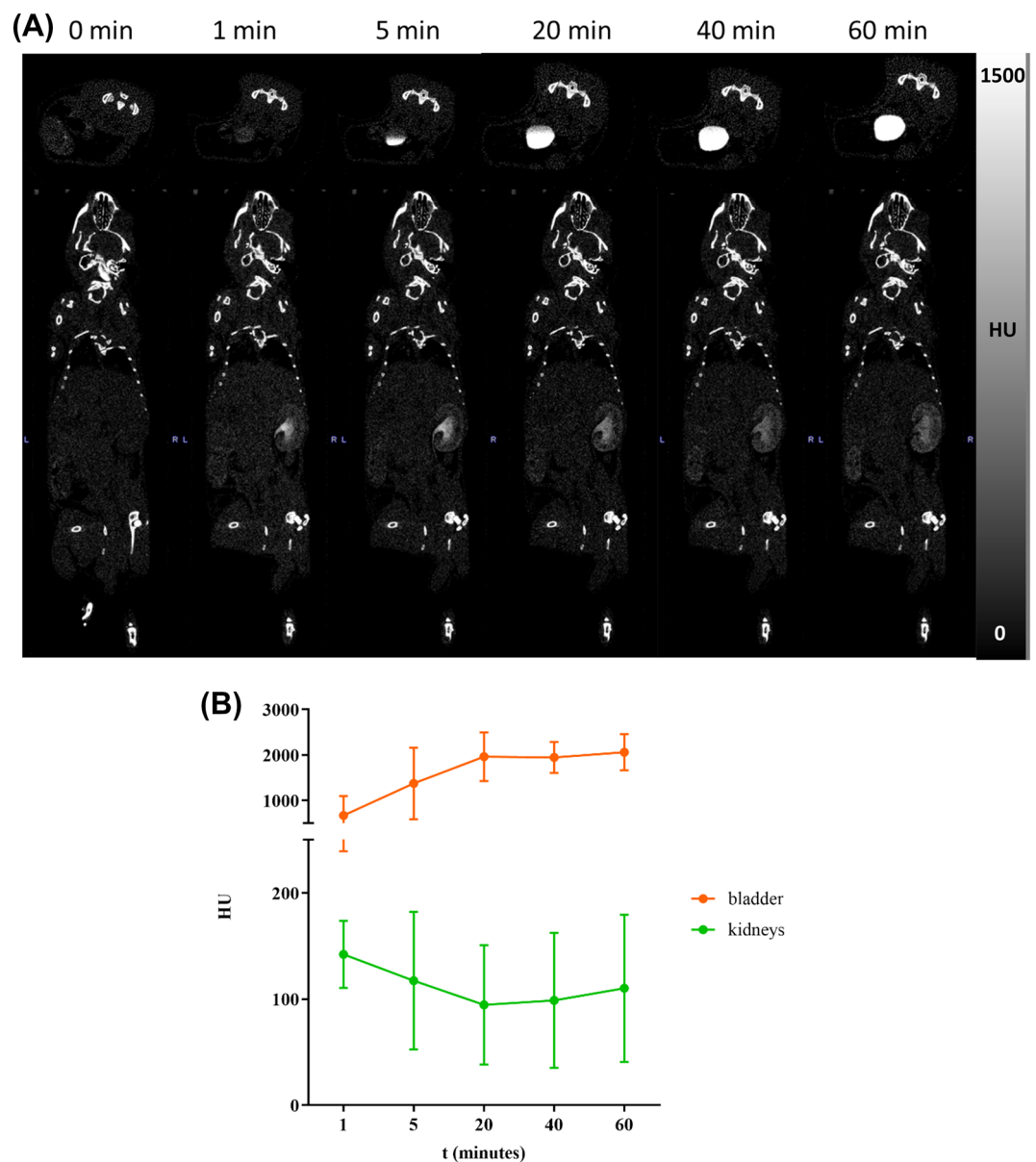


Figure 7. (A) In vivo CT imaging after i.v. administration of 1.2 mmol/kg of Bi-HPDO3A. Bladder and kidneys CT contrast are displayed. (B) VOIs analysis on bladder and kidneys for a dose of 1.2 mmol/kg of Bi-HPDO3A.

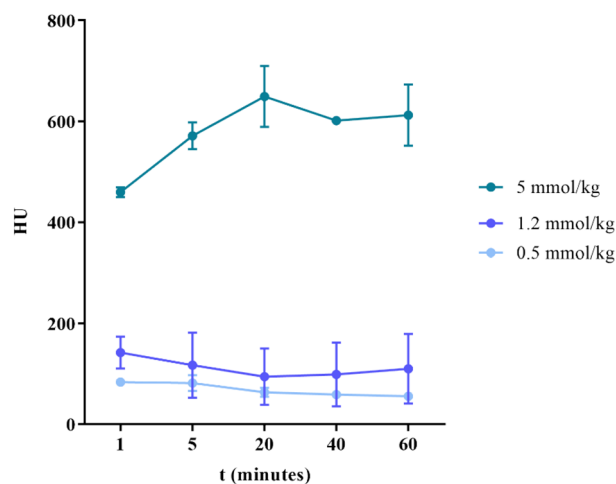


Figure 8. Dynamics of the kidney CT contrast for the three different injected doses of Bi-HPDO3A.

agents, with the more hydrophilic Bi-HPDO3A complex that showed a faster renal clearance. To preliminarily investigate the in vivo acute toxicity of the new compound in the main excretory organ, HE staining of the kidneys of mice injected with the highest dose (5 mmol/kg) of agent was performed. No tissue-damaging effects were found (Fig. S10), thus confirming the good safety profile of the new probe.

Conclusions

This study presents a novel bismuth-based potential CT contrast agent based on the HPDO3A ligand. The high X-ray attenuation coefficient of bismuth, its wide safety profile, and the well-known characteristics as chelating agent of HPDO3A, already clinically employed, makes it an excellent candidate for this purpose. Although the sub-optimal voltage (65 kV) of the available scanner, Bi-HPDO3A has proved to have a good potential as CT contrast agent for imaging kidneys and bladder. The high-water solubility of this agent led to a rapid renal excretion, faster than Iopamidol, thus reducing possible risks of toxicity caused by unwanted tissue accumulations. The results herein reported suggest further investigations. Multimeric versions of this ligand, or similar macrocyclic ligands forming neutral complexes with trivalent metals, have been already reported, which could improve detection sensitivity, in analogy to what has been done with iodinated agents^{23,24}. Furthermore, HPDO3A ligand is suitable of conjugation with chemicals for modulating and optimizing the biodistribution of the agent, thus opening new potential applications, in addition to image renal diseases.

Data availability

Data will be made available upon request to Rebecca Rizzo.

Received: 10 July 2023; Accepted: 18 September 2023

Published online: 05 October 2023

References

- De Marcillac, P., Coron, N., Dambier, G., Leblanc, J. & Moalic, J. P. Experimental detection of α -particles from the radioactive decay of natural bismuth. *Nature* **422**, 876–878 (2003).
- Ahenkorah, S. *et al.* Bismuth-213 for targeted radionuclide therapy: From atom to bedside. *Pharmaceutics* **13**, 1–25 (2021).
- Briand, G. G. & Burford, N. Bismuth compounds and preparations with biological or medicinal relevance. *Chem. Rev.* **99**, 2601–2658 (1999).
- Li, H., Yuan, S., Wei, X. & Sun, H. Metal-based strategies for the fight against COVID-19. *Chem. Commun.* **58**, 7466–7482 (2022).
- Griffith, D. M., Li, H., Werrett, M. V., Andrews, P. C. & Sun, H. Medicinal chemistry and biomedical applications of bismuth-based compounds and nanoparticles. *Chem. Soc. Rev.* **50**, 12037–12069 (2021).
- Gill, M. R. & Vallis, K. A. Transition metal compounds as cancer radiosensitizers. *Chem. Soc. Rev.* **48**, 540–557 (2019).
- Franchi, S., Di Marco, V. & Tosato, M. Bismuth chelation for targeted alpha therapy: Current state of the art. *Nucl. Med. Biol.* **226**, 25 (2022).
- Gomez, C., Hallot, G., Laurent, S. & Port, M. Medical applications of metallic bismuth nanoparticles. *Pharmaceutics* **13**, 1–26 (2021).
- Koç, M. M., Aslan, N., Kao, A. P. & Barber, A. H. Evaluation of X-ray tomography contrast agents: A review of production, protocols, and biological applications. *Microsc. Res. Tech.* **82**, 812–848 (2019).
- Lusic, H. & Grinstaff, M. W. X-ray-computed tomography contrast agents. *Chem. Rev.* **113**, 25 (2013).
- Algethami, M., Feltis, B. & Geso, M. Bismuth sulfide nanoparticles as a complement to traditional iodinated contrast agents at various X-ray computed tomography tube potentials. *J. Nanomater. Mol. Nanotechnol.* **06**, 2–10 (2017).
- Oh, M. H. *et al.* Large-scale synthesis of bioinert tantalum oxide nanoparticles for X-ray computed tomography imaging and bimodal image-guided sentinel lymph node mapping. *J. Am. Chem. Soc.* **133**, 5508–5515 (2011).
- Rabin, O., Perez, J. M., Grimm, J., Wojtkiewicz, G. & Weissleder, R. An X-ray computed tomography imaging agent based on long-circulating bismuth sulphide nanoparticles. *Nat. Mater.* **5**, 118–122 (2006).
- Tarighatnia, A. *et al.* Engineering and quantification of bismuth nanoparticles as targeted contrast agent for computed tomography imaging in cellular and animal models. *J. Drug Deliv. Sci. Technol.* **66**, 102895 (2021).

15. Fu, J. J. *et al.* Bismuth chelate as a contrast agent for X-ray computed tomography. *J. Nanobiotechnol.* **18**, 1–10 (2020).
16. Dai, G. *et al.* Small-molecule bi-DOTA complex for high-performance CT and spectral CT bioimaging. *Front. Oncol.* **12**, 1–11 (2022).
17. Hermann, P., Kotek, J., Kubiček, V. & Lukeš, I. Gadolinium(III) complexes as MRI contrast agents: Ligand design and properties of the complexes. *Dalt. Trans.* **9226**, 3027–3047 (2008).
18. Barge, A. *et al.* Synthesis of functionalised HP-DO3A chelating agents for conjugation to biomolecules. *Org. Biomol. Chem.* **7**, 3810–3816 (2009).
19. Laurent, S., Vander Elst, L., Henoumont, C. & Muller, R. N. How to measure the transmetallation of a gadolinium complex. *Contrast Media Mol. Imaging* **5**, 305–308 (2010).
20. Csajbo, Á., Baranyai, Z., Platzek, J., Radu, B. & Scha, M. Equilibrium, ¹H and ¹³C NMR spectroscopy, and X-ray diffraction studies on the complexes bi (DOTA)- and Bi (DO3A-Bu). *Inorg. Chem.* **42**, 2342–2349 (2003).
21. Nair, A. & Jacob, S. A simple practice guide for dose conversion between animals and human. *J. Basic Clin. Pharm.* **7**, 27 (2016).
22. Bourin, M., Jolliet, P. & Ballereau, F. An overview of the clinical pharmacokinetics of X-ray contrast media. *Clin. Pharmacokinet.* **32**, 180–193 (1997).
23. Lohrke, J. *et al.* Preclinical profile of gadoquatrane: A novel tetrameric, macrocyclic high relaxivity gadolinium-based contrast agent. *Invest. Radiol.* **57**, 629–638 (2022).
24. Di Gregorio, E., Ferrauto, G., Gianolio, E. & Aime, S. Gd loading by hypotonic swelling: An efficient and safe route for cellular labeling. *Contrast Media Mol. Imaging* **8**, 475–486 (2013).

Acknowledgements

The Italian Ministry for Education and Research (MIUR) is gratefully acknowledged for yearly FOE funding to the Euro-BioImaging Multi-Modal Molecular Imaging Italian Node (MMMI).

Author contributions

Conceptualization R.R., M.C., E.T., synthesis and characterization R.R. C.C., in vitro studies R.R. M.C., in vivo studies M.C., R.R., data processing R.R. writing—original draft preparation R.R., writing—review and editing R.R, M.C., E.T., supervision E.T. All authors have read and agreed to the published version of the manuscript.

Competing interests

The authors declare no competing interests.

Additional information

Supplementary Information The online version contains supplementary material available at <https://doi.org/10.1038/s41598-023-43031-y>.

Correspondence and requests for materials should be addressed to E.T.

Reprints and permissions information is available at www.nature.com/reprints.

Publisher's note Springer Nature remains neutral with regard to jurisdictional claims in published maps and institutional affiliations.



Open Access This article is licensed under a Creative Commons Attribution 4.0 International License, which permits use, sharing, adaptation, distribution and reproduction in any medium or format, as long as you give appropriate credit to the original author(s) and the source, provide a link to the Creative Commons licence, and indicate if changes were made. The images or other third party material in this article are included in the article's Creative Commons licence, unless indicated otherwise in a credit line to the material. If material is not included in the article's Creative Commons licence and your intended use is not permitted by statutory regulation or exceeds the permitted use, you will need to obtain permission directly from the copyright holder. To view a copy of this licence, visit <http://creativecommons.org/licenses/by/4.0/>.

© The Author(s) 2023